

ATTITUDE CONTROL OF FLEXIBLE LAUNCH VEHICLE USING ADAPTIVE NOTCH FILTER

Choong-Seok Oh and Hyochoong Bang

*Dept. of Aerospace Engineering,
Korea Advanced Institute of Science and Technology (KAIST)*

Abstract: Attitude control of a flexible launch vehicle is addressed in this study. A ground experimental model is developed for verification of different stabilization strategies. The experimental set up duplicates planar motion of flexible launch vehicles as a coupled hybrid dynamics of rigid body pitching motion and flexible vibration. In particular, adaptive notch filter, which updates filter parameters continuously from the sensor measurement, is implemented in real-time with experimental demonstration. The principal purpose of this study is, therefore, to verify the existing adaptive filter algorithm to investigate feasibility of actual implementation of the adaptation logic. Through experiment, it was shown that the adaptive filter stabilizes an uncertain system successfully in conjunction with thruster vector control actuation device using an air-thruster. *Copyright © 2005 IFAC*

Keywords: Attitude control, flexible launch vehicle, adaptive notch filter, ground experiment, thruster vector control

1. INTRODUCTION

Flexible rockets are represented by complicated dynamic characteristics due to structural vibration from the slender body shape, fuel sloshing, aerodynamic effect and engine gimbal dynamics (Greensite, 1970). The attitude command delivered to the TVC system being located usually at the end of the rocket main body is generated from the attitude angles and angular rates measured by inertial measurement unit (IMU). Sometimes, the IMU signal consists of not only rigid-body mode but also flexible vibrational modes. It is a well-known problem; sensor location and associated stability problem. In the launch vehicle attitude control system design, the instability due to structural feedback should be taken into account carefully.

There have been a number of papers and technologies associated with stabilization of flexible launch vehicles. The stabilization techniques are largely based upon structural filters such as low-pass, high-pass, band-pass, and notch filters (Ljunge and Hall, 1984). Sometimes combinations of filters of different structures are used to meet the stability and performance requirement. Intensive research effort has been made also for a notch filter design to minimize the effect of structural vibration near the natural frequency range (Wie and Byun, 1989; Rao and Kung, 1984; T-Romano and Bellanger, 1988;

Regalia, 1991; Nehorai, 1985). The attitude control system design and associated filter design approaches are tested by computer simulation in general. Majority of research work rely on a mathematical model that suffers from modelling errors in real applications. Not much information and data are available for the actual implementation of filter design for actual launch vehicles. Research on active control for flexible launch vehicles by ground based experiment is attractive due to inherent advantages of experimental demonstration. Limitation of analytical approaches could be resolved in many aspects through experimental approaches. Basic principles of stabilization techniques such as low pass, band pass, and notch filters can be investigated easily through experimental demonstration with minimal cost. It may not be easy, however, to create similar environment that is close to actual launch environment. Also, gravity effect, friction, and other unmodelled error sources raise difficulties for the ground experiment. Establishing reasonable similarity between a ground model and actual launch vehicles is another key issue in ground experimental study. Despite such difficulties, preliminary research on the ground still provides huge benefits overcoming the risk involved with actual flight phase. In this study, attitude controller design for an experimental ground launch vehicle model is investigated. The principal objective is to examine conventional stabilization filters and test the

performance by experimental demonstration. It is not the main goal here to design a new control law, but to verify conventional control approaches. In particular, adaptive notch filter is actually applied to the real plant. For this goal, a ground hardware testbed is developed with sensors and actuators. The sensor include angular rate sensor. Real-time control is applied for attitude maneuver and vibration control of the launch vehicle model. Adaptive notch filter is implemented and tested in conjunction with closed-loop feedback control loop. This paper consists of several sections; in section 2, ground experimental model is described in detail; section 3 discusses generic control laws design approaches for the stabilization of flexible launch vehicles; in section 4, the experimental results are presented. Finally, the paper presents the some conclusions in section 5.

2. GROUND EXPERIMENTAL MODEL

2.1 Generic launch vehicles

Governing equations for flexible launch vehicles are fairly well known already. Main issues include various dynamic effects such as gravitation, thrusters, flexibility, fuel sloshing and engine gimbal inertia effect. Graphical representation and notations to build dynamic motions for a flexible launch vehicle is presented in Fig. 1. The l_a is distance from nose of vehicle to origin of body axis system, l_α is distance from center of pressure in pitch plane to origin of body axis system, l_o is distance from c.g. of vehicle to sensor location, l_c is distance from origin of body axis system to engine swivel point.

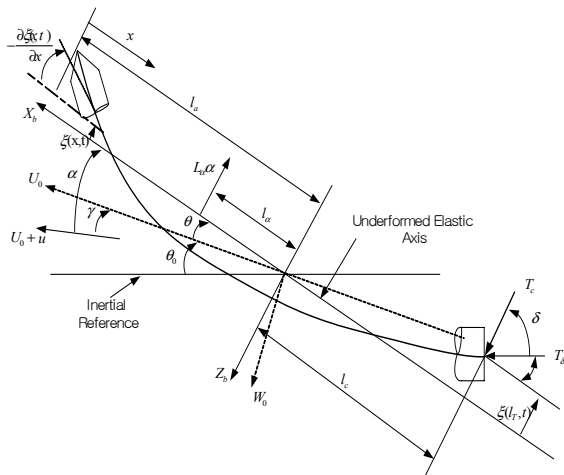


Fig. 1. Free-body diagram for a launch vehicle with flexible motion

2.2 Experimental model design

The experimental model designed in this study is used to test the basic attitude stabilization control approaches presented in the following section. In particular, in order to design a model that can simulate actual launch vehicle dynamics to the best extent possible the following conditions should be considered;

- Friction effect should be minimized to effectively produce structural motion.

- Appropriate sensors and actuators should be available to implement real-time control experiment.
- External disturbance effect should be generated to cover various disturbance sources in particular structural and other inputs in the form of vibration.

The schematic explanation of the experimental set-up is presented in Fig. 2. A flexible structure with sufficient flexibility sitting on top of air-pads is used as a launch vehicle model. The whole structure is floating on a granite table to provide frictionless dynamic environment. Due to the limited space for experiment, the motion of the model is limited to rotational motion without planar translational motion. One end of the structure is pinned to a supporting structure to prevent translational motion. Attached to the end of the structure module is TVC(Thrustor Vector Control) module as a duplication of a common subsystem of generic liquid engine powered launch vehicles. The picture of TVC module is presented in Fig. 3. The TVC module uses dry air as propellant being supplied by compressed air tank through a flexible tube. The thruster valve itself is actuated by a DC servo motor to produce engine gimbal deflection angle effect. The valve actuation is controlled in on-off mode by solenoid valves driven by 24V power source. The valve on-time is controlled by an output board connected to the main processor. The actual picture for the experimental model including TVC module is also displayed in Fig. 4. Reaction effect due to engine inertia, fuel sloshing dynamics and aerodynamic torque are considered as disturbances. The disturbance effect in the form of

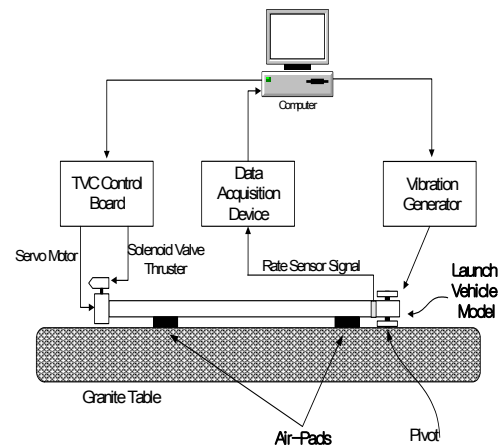


Fig. 2. Schematics for the ground model for experiment

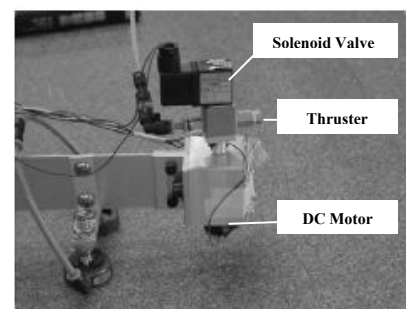


Fig. 3. Thruster vector control module

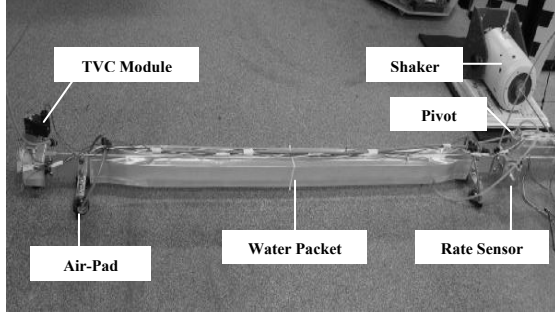


Fig. 4. Ground experimental set-up with TVC actuator

bending moment is generated piezoceramic actuators attached to the end of the structure or shaker. In fact, arbitrary disturbance can be implemented by adjusting input signal to the disturbance excitation actuator. The excitation frequency is selected as band-limited Gaussian noise (0-50Hz). The water packets are attached to each side to represent the launch vehicle model mass variation.

2.3 Modeling by finite element method

In order to conduct preliminary simulation study and conduct baseline controller design, a finite dimensional mathematical model for the ground model dynamics is established first as shown in Fig. 5. Since the model dynamics consist of hybrid coordinates of rigid body motion and flexible vibration, the governing equations of motion are described by a hybrid form of ordinary and partial differential equations of motion (Meirovitch, 1967; Wie, 1998).

$$I_c \ddot{\theta} + \int_{l_0}^l \rho x (x \ddot{\theta} + \frac{\partial^2 y}{\partial t^2}) dx + m_t l (\ddot{\theta} + \frac{\partial^2 y}{\partial t^2} \Big|_l) = u \quad (1)$$

$$\rho (x \ddot{\theta} + \frac{\partial^2 y}{\partial t^2}) + EI \frac{\partial^4 y}{\partial x^4} = 0, \quad l_0 < x < l$$

where I_c represents moment of inertia of the center body, θ denotes rotation angle of the whole structure, and m_t represents tip mass in particular the mass of the tip TVC system. Also, u is control torque developed by TVC or disturbance, ρ, EI represent linear mass density as well as elastic rigidity of the flexible structure, and $y(x, t)$ denotes flexural deflection. Also, the following boundary conditions are satisfied for the given model:

$$y(x, t) = \frac{\partial y(x, t)}{\partial x} = 0, \quad \text{at } x = l_0$$

$$EI \frac{\partial^2 y}{\partial x^2} = 0, \quad EI \frac{\partial^3 y}{\partial x^3} = m_t (l \ddot{\theta} + \frac{\partial^2 y}{\partial t^2}), \quad \text{at } x = l$$

For simulation study and control system analysis, the original infinite dimensional system can be discretized into a finite dimensional system. Finite element method is used in this study to construct the following system of ordinary differential equations (Meirovitch, 1967; Kwon and Bang, 2000):

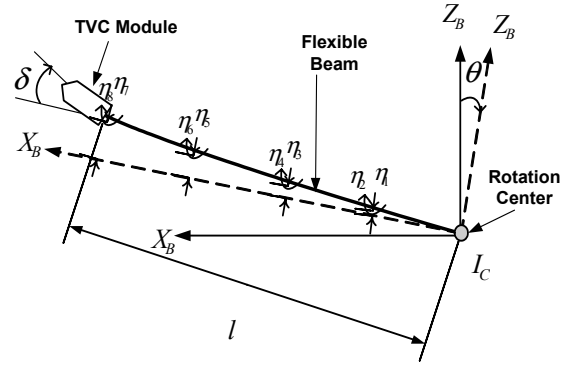


Fig. 5. Finite element model

$$\begin{bmatrix} I_t & M_{\theta\eta} \\ M_{\eta\theta} & M_{\eta\eta} \end{bmatrix} \begin{Bmatrix} \ddot{\theta} \\ \ddot{\eta} \end{Bmatrix} + \begin{bmatrix} I_t & M_{\theta\eta} \\ M_{\eta\theta} & M_{\eta\eta} \end{bmatrix} \begin{Bmatrix} \theta \\ \eta \end{Bmatrix} = \begin{bmatrix} L & 1 \\ 0 & 0 \\ 1 & 0 \\ 0 & 0 \end{bmatrix} \begin{Bmatrix} u_{th} \\ u_{pz} \end{Bmatrix} \quad (2)$$

where u_{th} represents torque by air thruster while u_{pz} denotes input torque by piezoceramic actuators.

The structural element was partitioned into five elements and the model parameters are specified as $\rho = 0.27 \text{ kg/m}$, $EI = 30 \text{ GPa}$, $I = 7 \times 10^{-11} \text{ kgm}^2$, $m_t = 0.3 \text{ kg}$, and $l = 1.3 \text{ m}$. Both I_c and l_0 are neglected. Natural frequencies of the system are estimated using the finite element model. The first three natural frequencies also identified by modal testing also. They turn out to be approximately 2.3 Hz, 7.5Hz, and 20Hz, respectively. Also, modal testing with FFT analysis was performed to estimate the natural frequencies. There are some discrepancies between the natural frequencies by analytical model modal testing. It is believe that unmodelled dynamics such as friction, disturbance due to air tube, and uncertain inertia properties of the experimental model created such discrepancies.

3. CONTROL APPROACH OF FLEXIBLE LAUNCH VEHICLES

Brief review on general approaches for the stabilization of flexible launch vehicles is presented. They are frequently used in actual applications and provide motivation for the main objective of this study. General stabilizing controllers are applied to the ground experimental model for real-time experiment. Numerous papers, too many to list here, are already available on the stabilization of flexible structures. One of the most general form of the filters is a second-order filter. Various filter structures can be realized by combination of the general second order filter. The minimum-phase second-order filter can be described in Laplace domain as (Wie and Byun, 1989)

$$H(s) = \frac{s^2 / \omega_z^2 + 2\zeta_z s / \omega_z + 1}{s^2 / \omega_p^2 + 2\zeta_p s / \omega_p + 1} \quad (3)$$

where $\omega_z, \zeta_z, \omega_p$, and ζ_p are filter parameter to be designed to lead to different filters such as notch, bandpass, low-pass, high-pass, and phase-lead, lag filters. The pole-zero patterns of the filter in Eq. (3) are important elements determining the performance of the filters.

3.1 Notch filter

In general, the notch filter can be designed by $\omega_p = \omega_z$ condition in Eq. (3). The minimum or maximum gain of the filter is obtained from $\omega_p = \omega_z$ such that $K_{\max} = 20 \log_{10}(\zeta_z / \zeta_p)$. Maximum phase lead occurs at a frequency determined by ζ_z and ζ_p .

This approach is to place poles or zeros of the compensator near flexible modes with relative small phase or gain margin. Such approach usually leads to increase in gain or phase margin. If exact knowledge of the frequency of the flexible modes is unknown, then performance of the controlled system tends to degrade drastically.

3.2 Adaptive notch filter

As mentioned above, performance of the notch filter is sensitive to modeling errors. In order to overcome such constraint, an adaptive notch filter using the sensor output signal to exactly estimate actual system frequency could be considered. The design parameters of the notch filter are updated continuously for exact matching with actual system parameters. As a consequence, adaptive notch filter is expected to produce much improved performance in the presence of modeling error. The main resource for the notch filter design is from Regalia (1991) and Nehorai (1985).

In this study, the adaptive notch filter is applied to actual real-time experimental study for the closed-loop feedback control experiment. Rao and Kung (1984) proposed the following form of a notch filter in the z-domain

$$H(z) = \frac{(1 - r_1 e^{j\phi} z^{-1})(1 - r_1 e^{j\phi} z^{-1})}{(1 - \gamma r_1 e^{j\phi} z^{-1})(1 - \gamma r_1 e^{j\phi} z^{-1})} \quad (4)$$

$$= \frac{1 - 2r_1 \cos \phi z^{-1} + r_1^2 z^{-2}}{1 - 2\gamma r_1 \cos \phi z^{-1} + \gamma^2 r_1^2 z^{-2}}$$

But the filter architecture in Eq. (4) is not most appropriate to apply the adaptive notch filter algorithm, so the following notch filter for adaptation has been proposed by Regalia

$$H(z) = \frac{1 + k_0(1 + k_1)z^{-1} + k_1 z^{-2}}{1 + a_0(1 + a_1)z^{-1} + a_1 z^{-2}} \quad (5)$$

In order to match Eq. (5) with Eq. (4), it should be satisfied that

$$a_0(1 + a_1) = \gamma k_0(1 + k_1) \quad (6)$$

$$a_1 = \gamma^2 k_1$$

Hence, they can be reduced into

$$a_0 = \frac{\gamma k_0(1 + k_1)}{1 + \gamma^2 k_1} \quad (7)$$

For implementation of adaptive notch filters, the number of parameters to be adapted should be

maintained minimum. If we assume γ is equal to 1, the parameters a_1, a_2 can be expressed in terms of k_1, k_2 such as

$$a_1 = \gamma^2 k_1 \cong \gamma k_1 \quad (8)$$

$$a_0(1 + a_1) = \gamma k_0(1 + k_1) \cong k_0(1 + k_1)$$

As a consequence,

$$a_0 = k_0$$

holds true and Eq. (5) can be rewritten as

$$H(z) = \frac{1 + k_0(1 + k_1)z^{-1} + k_1 z^{-2}}{1 + k_0(1 + \gamma k_1)z^{-1} + \gamma k_1 z^{-2}} \quad (9)$$

In general, better performance of a notch filter is ensured when zeros are located on the unit circle. Hence in Eq. (9), the parameter k_1 is set equal to unity, and it can be simplified as a function of γ and k_0 in the following form;

$$H(z) = \frac{N(z)}{D(z)} = \frac{1 + 2k_0 z^{-1} + z^{-2}}{1 + k_0(1 + \gamma)z^{-1} + \gamma z^{-2}} \quad (10)$$

In this study, γ lies between 0.9 and 0.99, and if it is close to 1 then the bandwidth becomes narrow.

Suppose the input signal to the notch filter is denoted as $u(n)$. Hence the filter output signal can be expressed as

$$y(n) = x(n) + 2k_0 x(n-1) + x(n-2) \quad (11)$$

where $x(n)$ represents a signal passing through the denominator of the filter, i.e.,

$$x(n) = \frac{1}{D(z)} u(n) \quad (12)$$

Now, in order to design the adaptation algorithm a cost function for optimization is proposed as follows;

$$E(n) = \sum_{k=0}^n \lambda^{n-k} y^2(k) \quad (13)$$

where λ represents a forgetting factor being less than unity. By using Eqs. (11) and (12), Eq. (13) can be modified into

$$E(n) = \sum_{k=0}^n \lambda^{n-k} [A(k)k_0 + B(k)]^2 \quad (14)$$

where each parameter is defined to be

$$A(k) = 2x(k-1), \quad B(k) = x(k) + x(k-2)$$

The cost function in Eq. (13) is minimized by a design parameter k_0 such that $\partial E / \partial k_0 = 0$, which leads to the following relationship

$$k_0 = - \frac{\sum_{k=0}^n \lambda^{n-k} A(k)B(k)}{\sum_{k=0}^n \lambda^{n-k} A^2(k)} = - \frac{C(n)}{D(n)} \quad (15)$$

where the new parameters satisfy

$$C(n) = \lambda C(n-1) + A(n)B(n)$$

$$D(n) = \lambda D(n-1) + A^2(n)$$

Since the notch poles are located within a unit circle, the parameter k_0 also lies in the range $k_0 \in [-1, 1]$. Consequently, the natural frequency of the bending vibration of the flexible structure can be estimated using the sampling time (Δt) in the following form:

$$\hat{\omega}(n) = \frac{\cos^{-1}[-k_0(n)]}{\Delta T} \quad (16)$$

The natural frequency is updated continuously according to Eq. (16). The parameter $k_0(n)$ is essentially driven by sensor signal.

4. EXPERIMENTAL RESULTS

The adaptive notch filter algorithm has been applied in actual experimental demonstration. The overall functional block diagram for the experimental set up is presented in Fig. 6. The angular rate of the whole structure is measured by an angular rate sensor through A/D converter at 200Hz sampling rate. The angle information is derived by directly integrating the angular rate signal. The central processing unit is Pentium-III 866MHz processor which computes control signal with digital filter. The thruster module is actuated by a DC servo motor for which angular displacement is controlled by an external motor controller. The motor controller itself is commanded by computer output. In this study, a TVC actuator is used to generate feedback control torque required. Technically it was difficult to handle the disturbance effect caused by air tube connected to the TVC actuator. Command for TVC actuator is issued at 25Hz. The A/D, and D/A board have 12-bit resolution in discretization. Piezoceramic actuator generates sinusoidal disturbing bending moments in order to simulate launch environment. The control signal to the piezoceramic actuator can be arbitrarily manipulated by function generators or S/W programmed command.

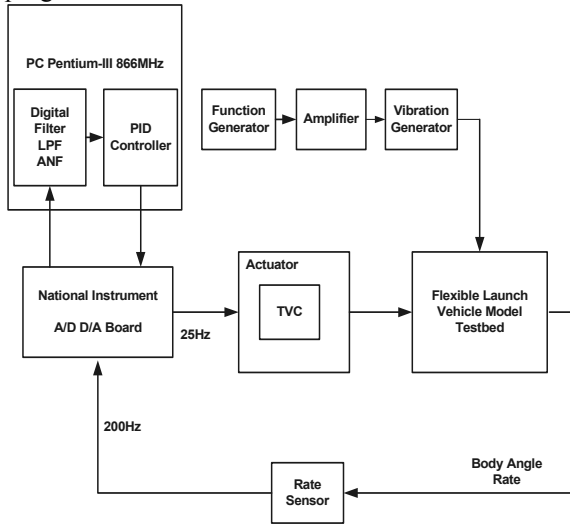


Fig. 6. Functional block diagram for the overall experimental set-up

The PID-type controller ($K_p = 100$, $K_I = 0.5$, $K_D = 80$) is applied to experiment. Figure 7 shows experimental results with a low-pass filter only without a notch filter. The low-pass filter is a second-order filter with 2.5Hz cut-off frequency to control modes higher than the second mode. The resultant closed-loop response shows undamped oscillation due to the first mode. The corresponding actuator command is also oscillatory due to insufficient gain and phase margins around the external disturbance close to the first mode. As a remedy for this situation,

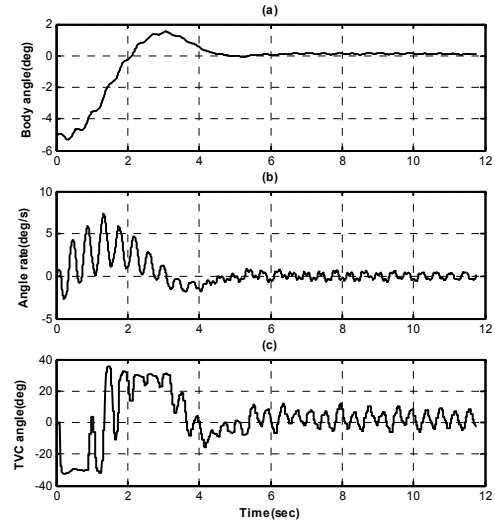


Fig. 7. Experimental results using low pass filter

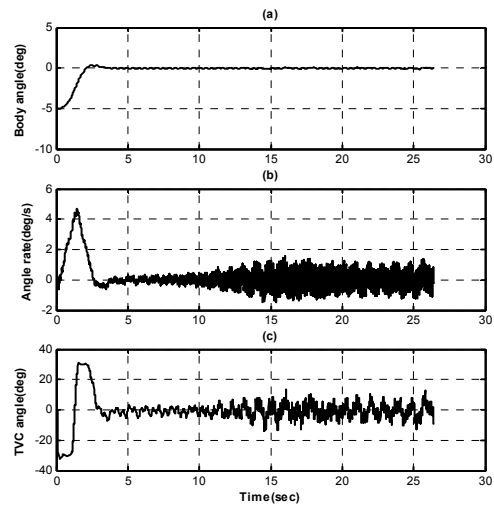


Fig. 8. Experimental results with a notch filter (incorrect notch filter parameter)

a low-pass filter can be augmented, but it will cause sluggish rigid body response and poor improvement in the stability margins for the first mode. Next, experimental results with a notch filter augmented are presented in Fig. 8. The filter parameter is initialized with some error. The actual first mode natural frequency is 2.3Hz while the notch filter frequency is selected as 2.6Hz. Even if the parameter error is just 12%, the responses show

residual oscillations due to the incorrect notch filter parameter. Perfect notch action does not take place in this case which results in significant oscillation in angular rate response. It would degenerate into instability easily under slight disturbance. Figure 9 presents experimental results with an adaptive notch filter implemented in the closed-loop. As it can be shown, all the responses are stabilized at the steady state with adaptive notch filter. The initial filter parameter is set to 1.5 Hz with as big as 34% magnitude error, but it converges quickly to the true system natural frequencies. The large parameter error is shown to be overcome effectively in the experiment. The constants in the notch filter parameter are set to $\gamma = 0.92$ and $\lambda = 0.98$,

respectively. These parameters, as mentioned already, are so important determining the notch filter performance. As the parameter γ approach unity, the notch action becomes dramatic, thus accurate estimation of the notch filter parameter is so critical. If the forgetting factor is so small, the estimation performance is degraded. But if it is too large, the performance is also degraded for the case of time varying parameter estimation. In the experimental investigation, the selection of an appropriate forgetting factor is important for the resulting performance of the notch filter. Figure 10 shows the experimental results of estimated frequency for the bending mode.

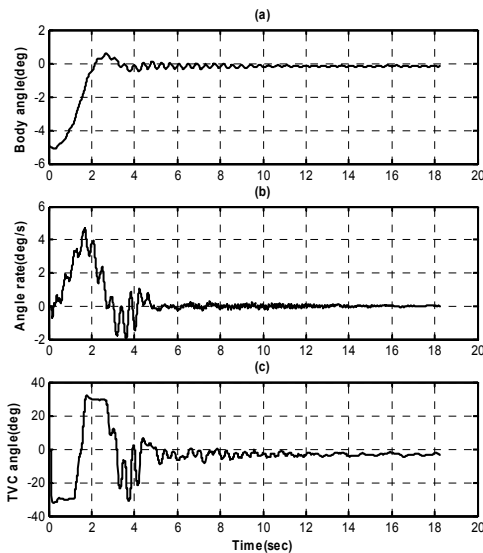


Fig. 9. Experimental results with adaptive notch filter

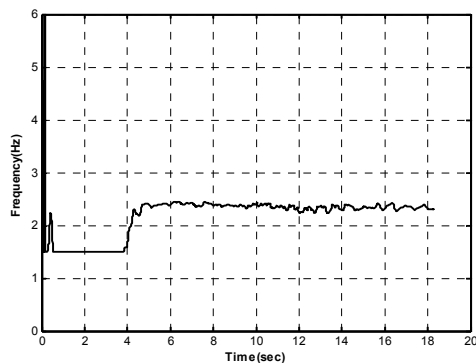


Fig. 10. Estimated filter parameter response by adaptive notch filter algorithm

5. CONCLUSION

A flexible launch vehicle ground model has been developed with experimental verification. The model is used for demonstration of real-time active attitude control and stabilization. In particular, adaptive notch filter algorithm was implemented in order to overcome the weakness of a simple low-pass filter compensator in vibration control of higher flexible modes. Experimental results illustrate the useful feature of the adaptive notch filter stabilizing the attitude response of the launch vehicle model. A large initial error in the filter parameter is accommodated effectively by the adaptation

algorithm. Therefore, this study provides demonstration of the feasibility of applying a notch filter with real-time adaptation. Further study should be considered for the case of multi-mode with corresponding multi-mode notch filter design.

ACKNOWLEDGEMENT

The present works is supported by KSLV-I development program operated by Korea Aerospace Research Institute. The financial and technical support by Dr. Hyeongdon Choi is fully appreciated.

REFERENCES

- Choi, H.D., and Bang, H.C. (2000). An Adaptive Control Approach to the Attitude Control of a Flexible Rocket. *Control Engineering Practice*, Aug., 1003-1010.
- Gaylor, R., Schaeperkoetter, R. L. and Cunningham, D.C. (1967). An Adaptive Tracking Filter for Bending-Mode Stabilization. *AIAA Journal of Spacecraft and Rockets*, 4, 573-577.
- Greensite, A. L. (1970). *Analysis and Design of Space Vehicle Flight Control Systems*. Spartan Books, New York.
- Joshi, S.M. (1989). *Control of Large Flexible Space Structures*. Springer-Verlag.
- Kwon, Y., and Bang, H. C. (2000). *The Finite Element Method using MATLAB*, CRC Press.
- Ljunge, L., and Hall, L. (1984). S19 Guidance of the Black Brant X Sounding Rocket. *AIAA Journal of Guidance, Control, and Dynamics*, 7, 156-160.
- Nehorai, A. (1985). A Minimal Parameter Adaptive Notch Filter With Constrained Poles and zeros. *IEEE trans on ASSP*, 33, 983-996.
- Meirovitch, L. (1967). *Analytical Methods in Vibrations*, Macmillan Company, pp. 126-143. New York.
- Rao, D.V., and Kung, S.Y. (1984). Adaptive Notch Filtering for the Retrieval of Sinusoids in Noise. *IEEE Trans. On Acoustic, Speech, Signal Processing*, 32, 791-802.
- Regalia, P.A. (1991). An Improved Lattice-Based Adaptive IIR Notch Filter. *IEEE Trans. on Acoustic Speech, Signal Processing*, 39, 2124-2128.
- T-Romano, J.M., and Bellanger, M. (1988). Fast Least Square Adaptive Notch Filtering. *IEEE Trans. on Acoustic Speech, Signal Processing*, 36, 1536-1540.
- Wie, B. (1998). *Space Vehicle Dynamics and Control*. AIAA Education Series, AIAA.
- Wie, B., and Byun, K.-W. (1989). New Generalized Structural Filtering Concept of Active Vibration Control Synthesis. *AIAA Journal of Guidance, Control, and Dynamics*, 12, 147-154.